Third-day trip 2 road log, geomorphic and hydrologic response in Estancia Basin to late Pleistocene and Holocene climate change

Roger Y. Anderson and Bruce D. Allen

1999, pp. 75-82. https://doi.org/10.56577/FFC-50.75

in:

Albuquerque Geology, Pazzaglia, F. J.; Lucas, S. G.; [eds.], New Mexico Geological Society 50 th Annual Fall Field Conference Guidebook, 448 p. https://doi.org/10.56577/FFC-50

This page is intentionally left blank to maintain order of facing pages.

THIRD-DAY, TRIP 2 ROAD LOG, GEOMORPHIC AND HYDROLOGIC RESPONSE IN ESTANCIA BASIN TO LATE PLEISTOCENE AND HOLOCENE CLIMATE CHANGE

ROGER Y. ANDERSON and BRUCE D. ALLEN

SATURDAY, SEPTEMBER 25, 1999

Assembly point: South end of parking lot of Hilton Hotel, Menaul and University, Albuquerque.
Departure time: 8:00 a.m.
Distance: 78.9 (with respect to the I-40 Sedillo Overpass)
Stops: 4; 1 optional stop

SUMMARY

Pluvial Lake Estancia, in Estancia basin (Fig. 3.2.1), responded dramatically and quickly to the extreme perturbations in climate that preceded and accompanied the Last Glacial Maximum (LGM). Highstand shorelines of the LGM are preserved as beaches, spits, and shoreline deposits around the basin margin. In the center of the basin, lake sediments document a change in salinity and lake level for virtually every century-scale shift in climate recognized in Greenland ice. The final pulse of glacial climate is preserved as a continuous, undissected beach ridge that extends for 19 mi. During the dry middle Holocene, winds cut nearly 100 playa basins into the old lake floor, forming lunettes higher than 100 ft. The route described in this guide, as noted in the road log, visits or passes these geomorphic, paleohydrologic, and geologic features. The log also gives brief summaries (bordered-text items) of key concepts or results of investigations carried out in Estancia basin. More information about the hydrology of Estancia basin can be found in Shafike and Flanigan (this volume).

To begin the trip, head east from the Albuquerque Hilton on I-40. The zero mileage point for the field trip is the overpass at the Sedillo Exit. Continue on I-40 about 28 mi to the second Moriarty exit and the junction with NM-41. Proceed south on NM-41.

FIGURE 3.2.1. Road log and index map indicating stops and showing shorelines of Lake Estancia highstands.

Mileage

0.0 Sedillo Overpass. Drainage divide of Estancia basin at crest of hill. **Set odometer to 0.0. 14.8**

14.8 Moriarty West, (Exit 196). **Take exit** and **turn right. 0.3**

15.1 Junction with NM-41. **Take NM-41 south. 2.9**

18.0 Highest shoreline elevation of Lake Estancia (6200 ft) is near the mouths of two major drainages (Buffalo Draw just ahead). A large gravel-bar complex can be seen to the east of the highway, and steeply dipping deltaic deposits are exposed in a gravel pit on the east side of the highway ahead. Beyond this point, the highway descends below the elevation of the high shorelines (6150–6200 ft) and continues south on the relict-lake-floor surface (elevation range 6100–6140 ft). **4.3**

22.3 A fairly continuous wave-cut scarp, corresponding to the highest shoreline of the lake, parallels the highway to the west. **2.2**

24.5 County Road A72. Church building at junction. **Turn west on CR-A72. 0.6**

25.1 CR-A72 begins crossing a series of ridges and swales corresponding to the high shorelines of Lake Estancia. An AMS-^{14}C date of 16.73 ± 0.17 ka was obtained from pelecypod shell in littoral deposits at gravel pit 1.25 mi west of NM-41 on north side of road (elevation 6200 ft). This date corresponds to the latter part of the LGM highstand of the lake, which began ~20 ka and lasted for about 5 ka. Fine-grained sediment and mollusks were preserved at this locality because it was situated in a small embayment and was protected from waves. **0.8**

25.9 **Turn left** (south) on section-line road and continue for 0.9 mi. **0.9**

26.8 **Turn right** (west) on unimproved road and continue for

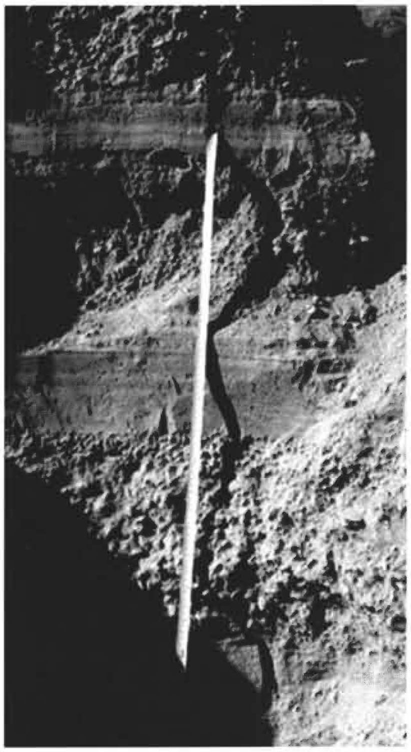

FIGURE 3.2.2. Exposure of transgressive/regressive lake-margin sediments in gravel quarry near MacIntosh.

0.7 mi to large gravel pit at the mouth of Cienega Draw. **0.7**

27.5 **Park in gravel pit for STOP 1.** Nearshore deposits associated with the glacial maximum highstand of Lake Estancia are exposed in numerous gravel pits along the western margin of the lake basin. A particularly thick section (~21 ft) of fine- and coarse-grained littoral deposits was preserved at this locality (elevation 6185 ft) because of its protected location and a large influx of sediment associated with stream discharge. Gravel pit exposures reveal landward-dipping, parallel-bedded gravels (beach bars) and several decimeter-scale, coarsening-upward sequences (Fig. 3.2.2), which probably reflect minor transgressive-regressive cycles of the lake. Ostracode zones suggest that sediments representing the entire LGM highstand of the lake are represented. Turn around in gravel pit and retrace route back to NM-41. **3.0**

30.5 **Turn right** (south) on NM 41 **0.2**

30.7 MacIntosh Post Office. **6.6**

37.3 Entering Estancia. Town settlement began between 1901 and 1904 after the railroad opened the region to homesteading. The town took its name form a nearby spring, which provided a "resting place." **0.9**

38.2 **Turn right** (west) on Highland Ave for 0.2 mi to the town park and site of a spring. Prior to large-scale pumping for irrigation, beginning in the 1940s, groundwater discharge occurred from a series of springs and seeps that extended in a line north and south of Estancia. The small pond at the park, now empty, has to be filled artificially because of groundwater withdrawals for irrigation. **0.2**

38.4 **Turn left** at entrance to park and continue south to NM-55. **0.2**

38.6 **Turn left** (east) on NM-55. **0.2**

39.0 **Turn right** (south) onto NM-41 and continue. **4.9**

43.9 Area of pumping and irrigation along highway. Cone of depression has ~40 ft of drawdown. **2.2**

46.1 Mouth of Manzano Draw drainage basin. Over the next ~1 mi, the highway crosses a gentle, topographic high that was formed by the deposition of sandy sediment at the mouth of Manzano Creek (Fig. 3.2.3). The sandy deposit forms a small delta that was been deposited during a brief expansion of the lake that occurred after the initial desiccation of Lake Estancia ~12 ka. An AMS-^{14}C date of 9.65 ± 0.07 ka from aquatic gastropod shell in a channel-fill deposit at the distal end of the delta provides a minimum age for the deposit. Geomorphic evidence for a brief expansion of the lake after 12 ka is also well preserved on the eastern side of the valley floor (discussed at Stop 3). The delta at Manzano Draw suggests that increased runoff and stream discharge played an important role in that highstand event. **0.4**

46.5 Manzano Draw channel (elevation 6120 ft). Manzano Draw (grassy reach between shrubs on delta sediments)

FIGURE 3.2.3. Photomap of Manzano Draw and delta.

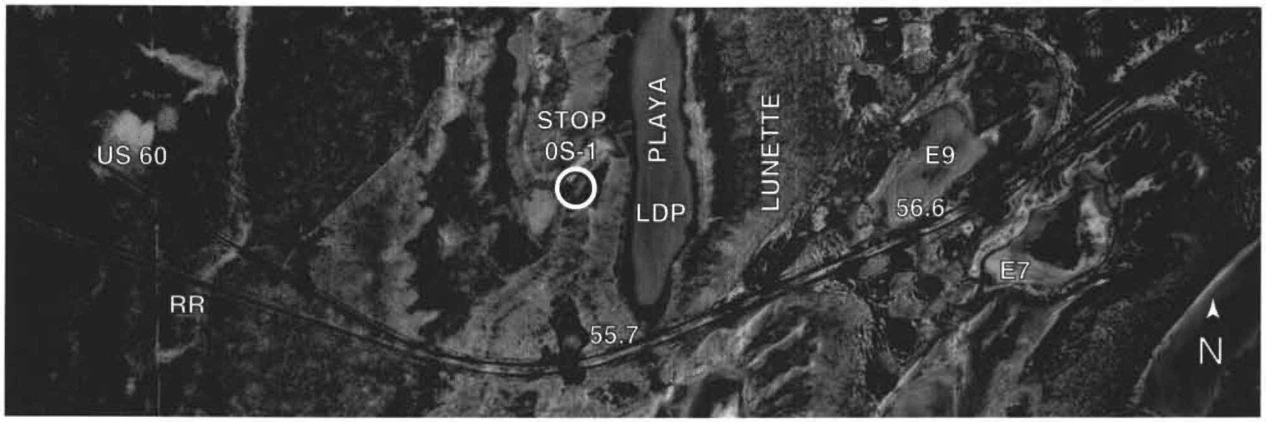

FIGURE 3.2.4. Photomap of southern end of Laguna del Perro. Location of optional stop OS-1.

drains some of the highest peaks in the Manzano Mountains to the west, and is one of a few, large drainages in Estancia basin that has created a stream channel that extends below the elevation of the high shorelines and onto the valley floor. Stream discharge events during the Holocene much larger than the event pictured in the 1973 air photo have dissected the delta, leaving a complex pattern of stream channels and delta remnants (Fig. 3.2.3). **3.2**

49.7 Junction with US-60. **Turn east on US-60.** Main line of the AT&SF Railroad to south of US-60. **1.2**

50.9 Note quartz sand dunes north of highway, resulting from deflation of nearshore sands associated with Lake Estancia. **0.3**

51.2 Entering Willard, founded in 1902. The town was named after the first son of a ATSF railroad promoter. **0.4**

51.6 Junction with NM-42. Continue east on US-60. To the south, NM-42 passes over the topographic sill (elevation 6340 ft) between Estancia basin and the closed, Piños Wells basin to the southeast (Fig. 3.2.1). The sill is about 14 mi to the south near the town of Cedarvale. LGM and later highstands in Estancia basin were ~130 ft lower than the sill. **0.4**

52.0 Hills ahead are clay dunes (lunettes) formed by deflation of the latest Pleistocene lake beds. **3.7**

55.7 Crossing southern end of Laguna del Perro (LDP; Fig. 3.2.4). Laguna del Perro is the largest of ~100 deflation basins that were carved into the valley floor during the mid-Holocene dry period of the American Southwest. LDP extends 7.5 mi to the north, and is about 0.6+ mi wide over much of its length. Material removed by deflation accumulated along the leeward side of the blowouts to form large dunes (lunettes) that rise up to 130-ft above the valley floor. The upper part of the latest Pleistocene lacustrine sequence is exposed in the walls of many of the blowouts. **0.9**

56.6 Passing small playa basin E9 and lunette on north side of highway. The playa surface on the south side of the highway (Playa E7), at a surface elevation of ~6040 ft, is one of the lowest in Estancia basin. Playa numbers were assigned by Bachhuber (1971).

Deflation basins and playas. Nearly 100 small basins were carved by deflation into the floor of the Pleistocene lake, sometime after the generation of the isolated gypsum-sand bedforms (Fig. 3.2.5a) and after the final lake highstand at ~10 ka. The down-wind margins of the wind-cut basins slope abruptly upward to the base of parabolic lunettes. The lunettes are composed of clay pellets with a high gypsum content, derived from underling lake sediments. After weathering, and upon wetting and drying, the pelletized sediment particles were transported across the deflated floor of the local basin by prevailing winds, and stacked into lunettes. Deflated surfaces beneath the playa sediments appear to be cut deeper on the west.

Vertical and oblique air photos (Fig. 3.2.5a, b) show that deflation of the playa-basins and creation of the lunettes occurred in two generations, as a result of two distinct climatic events. The older lunettes (first generation) are higher and farther removed from the modern playas. The deflation surface of 1st-generation blowouts has been cut several meters below the Pleistocene lake floor and is above modern playa level. On the eastern side of Estancia basin this cut surface extends a variable distance eastward from the margin of modern playas, and is capped by eolian materials derived from the 2nd generation of deflation. In some places a prominent bench forms the surface of these deposits. West of LDP, the cut surface of 1st-generation basins often extends west of the modern playa margin.

In the center of the Estancia basin, in the area of groundwater discharge, the 2nd-generation deflation surface is cut as much as 6.5 ft below the surface of modern playas, with depths of <1.5 ft in playas around the basin margin. Sediments within 2nd-generation basins are water-saturated to the playa surface and are composed largely of clay and finely divided gypsum derived from slopes around the playa, and abundant crystals of interstitially grown gypsum. Stratigraphic profiles of the playa fill reveal episodes of desiccation as well as zones of higher clay content and abundant resting cases (eggs) of *Artemia* (brine shrimp).

The onset of the 1st-generation of deflation occurred at ~7 ka, based on radiocarbon dates on gastropods collected at the base of first-generation lunette deposits at two separate localities. The age of playa fill deposits is poorly constrained because terrigenous organic materials in playa sediments are reworked from adjacent Pleistocene sediment and not suited for dating. A single date of 4.2 ka on *Artemia* eggs near the base of playa fill

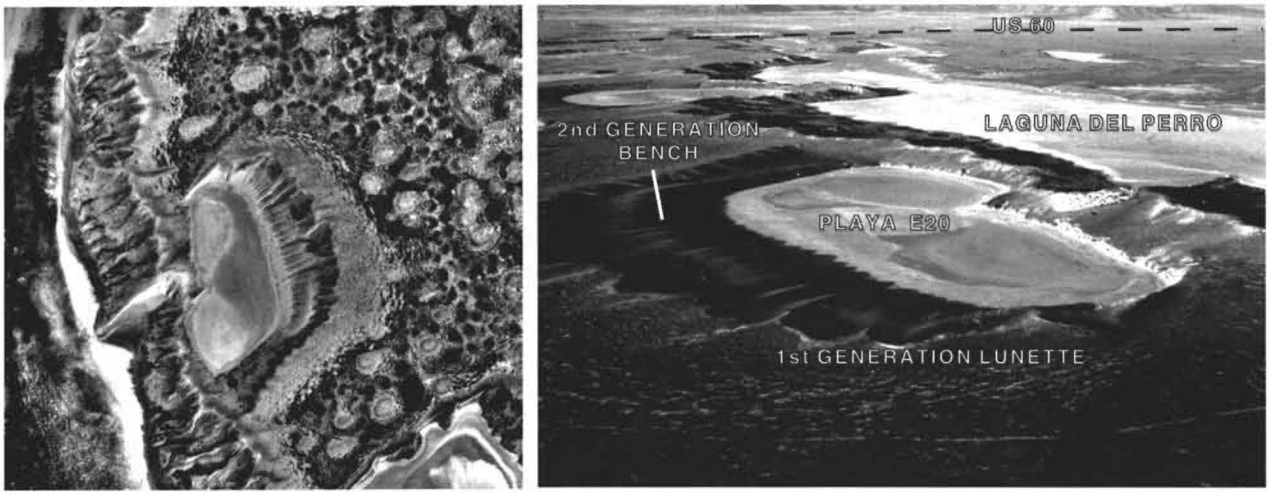

FIGURE 3.2.5a, b. Vertical and Oblique photos of Playa E20, showing isolated, dune-like gypsum bedforms, and two generations of deflation and lunettes.

suggests that deflation and low water levels persisted for several thousand years. **0.7**

57.3 Milepost 224. The small mounds forming the hummocky topography to the north of the highway (Fig. 3.2.5) are gypsiferous bedforms that predate the large deflation basins and lunettes (see Fig. 3.2.4), and formed from gypsum and carbonate that accumulated on the valley floor during desiccation of Lake Estancia ~12 ka. The isolated, dune-like bedforms contain 65–75% gypsum. **1.5**

58.8 Stop 4 will be at rest area on north side of highway (Fig. 3.2.6). **0.5**

59.3 Backslope of Playa E12 lunette on north side of highway (Fig. 3.2.7). **0.2**

59.5 Crossing another area dotted with low, gypsiferous bedforms on the north. Several railroad cuts pass through the isolated gypsum bedforms. The shape of the hummocky bedforms becomes linear and more complex near a gypsum beach ridge that lies to the east. **1.6**

61.1 Ridge extending north and south of highway (ridge-top elevation ~6112 ft) is a beach deposit composed primarily of gypsum. The gypsum beach ridge continues for ~20 mi along the east side of the lake and is at about the same elevation as the apex of the Manzano delta on the west side of the basin. The ridge reflects an abrupt and temporary return of the lake after complete desiccation at ~12 ka and will be discussed at Stop 3. **1.0**

62.1 Quartz sand dunes derived from deflation of littoral beach deposits on north side of highway. Begin climbing above valley floor. **0.5**

62.6 Undulations of the highway on the rising slope are gentle benches of the high shorelines of Lake Estancia. In this area the shorelines wrap around a north-trending bedrock high (Permian Glorieta Sandstone). **1.8**

64.4 Stop 2 will be at turnout on south side of highway. **0.8**

65.2 **Take dirt road north off of US-60. 1.3**

66.5 Road crosses a gravel spit (elevation 6150 ft). **Turn around at entrance to gravel pit on west side of road. STOP 2**. In this area, the high shorelines of Lake Estancia curve around a broad, gravelly ridge that extends northward into the lake basin, and then around a large spit composed of pebble gravel that extends northeastward ~2 mi from the northern tip of the gravel ridge (Fig. 3.2.8). Note well-developed shoreline terrace (elevation 6148 ft) on the flank of the spit. A date of 12.51 ± 0.09 ka was obtained from ostracodes in a thin clay bed at the base of the spit sequence. This date corresponds to a freshening event, identified in basin-center deposits that occurred during a major highstand between about 14 and 12 ka. Return to US-60. **1.3**

67.8 US-60. **Turn west** on highway. **0.8**

68.6 **Pull into turnout on south side of highway. STOP 3.**

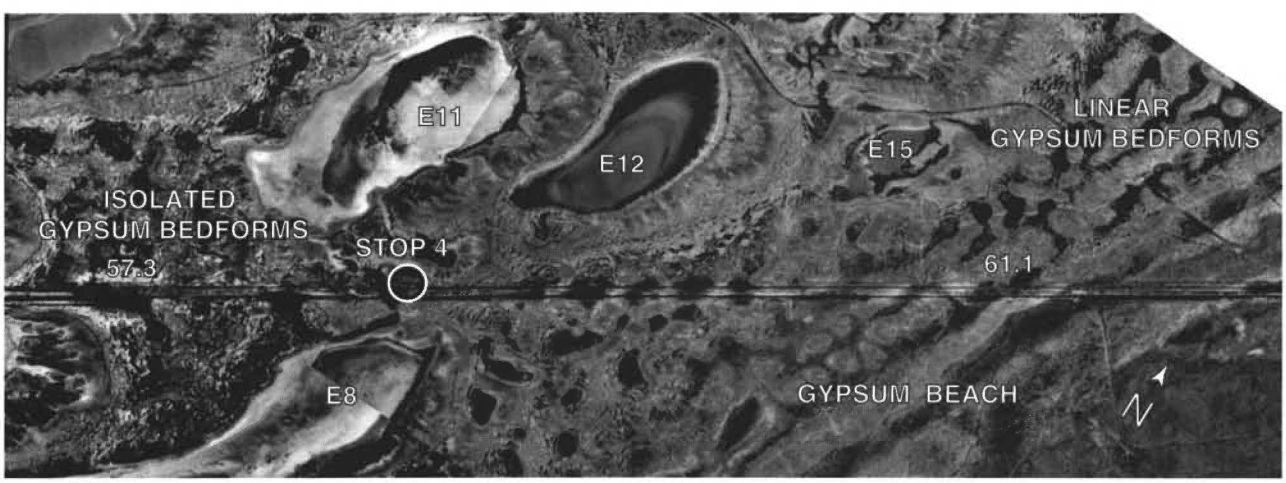

FIGURE 3.2.6. Photomap of eastern side of basin, showing location of Stop 4, isolated gypsum bedforms, and gypsum beach ridge.

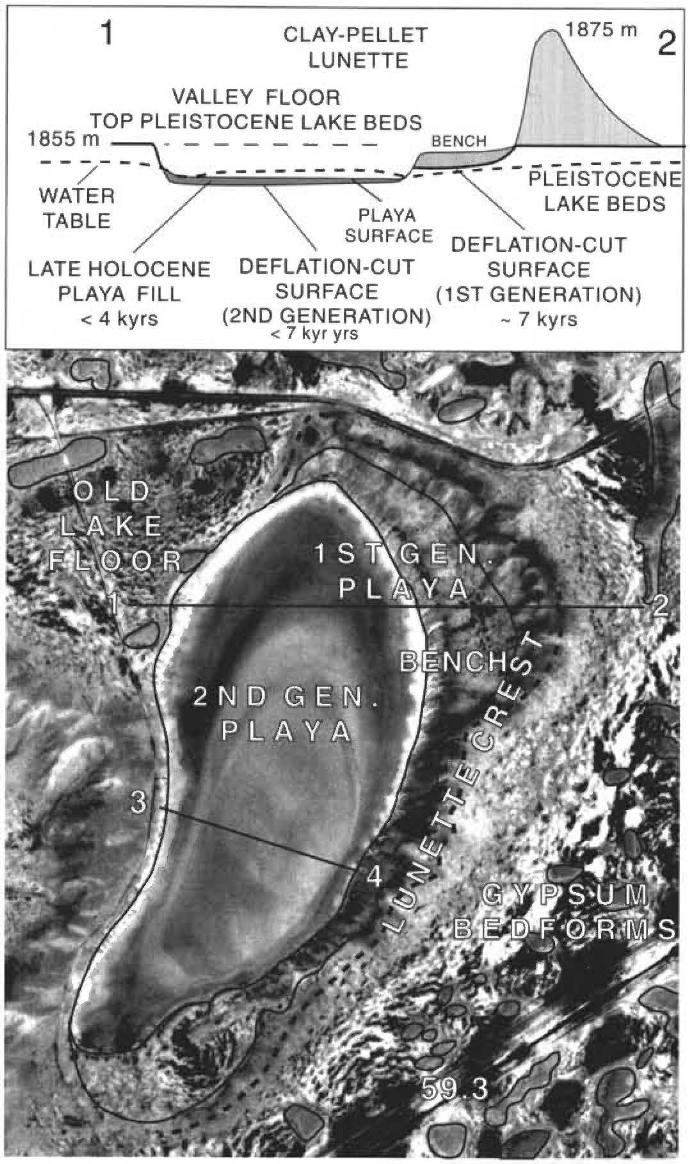

FIGURE 3.2.7. Photo and diagrammatic cross-section of Playa E12, showing location of transects and relation of lunette, bench, and playa sediment to deflation surfaces.

This stop is near the top of the high shorelines of Lake Estancia. The lake reached the elevation of the high shorelines on several occasions during the LGM (Fig. 3.2.1). At its largest extent, Lake Estancia covered an area of over 400 mi^2 and was a little over 130 ft deep. Another major highstand of the lake occurred at ~14 ka, during which two expansions of the lake are recorded. The second expansion of the lake did not rise above the elevation of the spit (6150 ft).

To the west, in the far distance, the Manzano Mountains are recharge areas for much of the groundwater discharged to the Pleistocene lake and that supports the modern playas. Surface discharge to the lake during lowstands and highstands was from the area of the foreground and from higher slopes that surround the basin. Blowouts and lunettes on the basin floor can be seen in the middle distance.

The linear, north-trending ridge along the eastern edge of the valley floor, about 3 mi to the west, is the gypsum beach ridge noted at Mile 61.1. The material forming this beach ridge was derived from the small, gypsum-sand bedforms scattered across the old lake floor after complete desiccation of Lake Estancia. The crest of the beach ridge is at a higher elevation than other bedforms (Fig. 3.2.9). Rising water during the rebirth and final expansion of Lake Estancia covered the gypsum bedforms, and, near the eastern shore, they were organized into linear shapes, bars, and beach ridges. Preservation of isolated, dune-like, gypsum-sand bedforms in areas distant from the eastern shoreline (Fig. 3.2.5a) suggests that expansion and contraction of the lake, which may correspond to the Younger Dryas climatic event, occurred abruptly.

Westward from the gypsum beach, Pleistocene lake sediments thicken and accumulated more continuously toward the basin center. Sediments in the transitional zone between the basin-center deposits and the high shorelines were sampled in a ~2.5-mi transect along US-60 just to the west of Stop 3. Individual clay beds in the basin-center sequence were traced to their marginal pinch-out using ostracode zones as identifiers (Fig. 3.2.9). The correlation with basin-center units shows that fine-grained beds deposited during major highstands of the lake extend a short distance marginward of the gypsum beach ridge, and then pinch out. Deposits of the littoral zone are dominated by gravel, except at special, protected localities (e.g. optional Stop OS-1 at Mile 30.9). In general, the three lithofacies depicted in Figure 3.2.9 represent deposition in offshore (clay), nearshore (sand), and beach (gravel) environments.

Stratigraphic relationships depicted in Figure 3.2.9 show that the shoreline of Lake Estancia did not fall below 7000 ft during lowstands, which corresponds to a minimum pool area of about 155 mi^2. Lake sediment accumulated continuously within this central area and the effects of fluctuating highstands and lowstands on sediment style and composition can be seen in the walls of deflation basins at stops along the return route. Proceed west on US-60. **3.3**

71.9 Gypsum beach ridge. **2.3**

74.2 **Pull into rest area. STOP 4.** Tan and gray lake beds are exposed in the distant, northern wall of the deflation basin to the north of US-60 (Fig. 3.2.6). These sediments are overlain by a thin, white horizon (Bachhuber's "B-zone") that formed in the large playa that covered the valley floor after initial desiccation of the lake. The small, gypsum bedforms and the lunettes discussed earlier occur on top of the white horizon. More accessible exposures are at Stop OS-1.

Some of the climatic-stratigraphic units within the lake bed sequence (Fig.3.2.10) can be seen beneath the small, truncated exposure of lake beds just to the north of deflated area immediately below the rest stop. This exposure is in the wall of a small, 1st-generation deflation basin that has been breached and now drains into Playa E11, altering its development as a second-generation playa basin.

Hydrology of the playas and playa basins. Water levels in test wells drilled near deflation basins reveal increasing hydraulic head with increasing depth (DeBrine, 1971), indicating upward-directed flow and

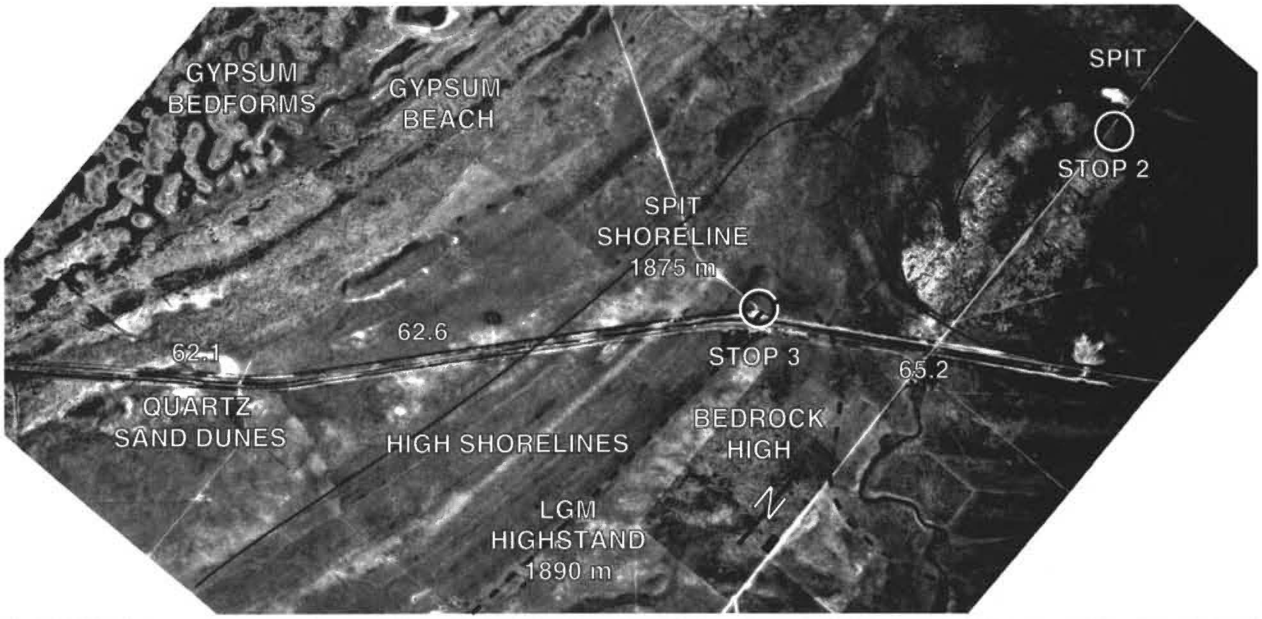

FIGURE 3.2.8. Photomap showing highest shorelines of Lake Estancia, bedrock high, and gravel spit to the north of highway, and location of Stops 2 and 3.

groundwater discharge. Piezometers in the playas, with screened intervals in permeable gypsum beds in underlying Pleistocene lake sediments, have potentiometric surfaces above playa level, with higher head in deeper strata. In the southern part of LDP this surface fluctuates in an annual cycle of ~3.0 ft; lowest in winter and highest in summer (Fig. 3.2.11).

Much of the groundwater is believed to originate in the Manzano Mountains to the west, move through permeable units in the valley fill and lake sediments, and discharge through the playas. Some groundwater also reaches the playas from the eastern side of the basin, probably through the valley fill. As part of current research, an east–west transect of piezometers was placed across Playa E12, on the eastern margin of the basin (Fig. 3.2.7). Seasonal changes in head across the E12 transect (Fig. 3.2.11) reveal a strong seasonal cycle and increased summer discharge in the west, and more constant seasonal flow reaching the playa from the east. Expression of the annual cycle in the western area of E12 playa, and the apparent basin-wide character of the strong annual cycle, suggest that even easternmost playas receive significant upward groundwater discharge through underlying stratigraphic units. Additional information about Estancia

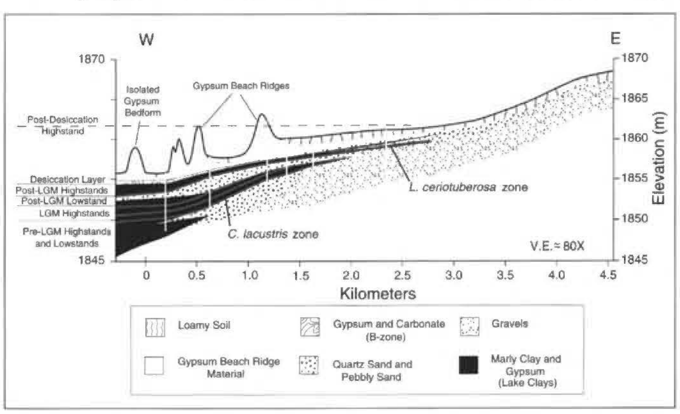

FIGURE 3.2.9 Cross section of eastern lake margin and pinch-out of Pleistocene lake sediments, showing relation to shoreline and gypsum beach ridge.

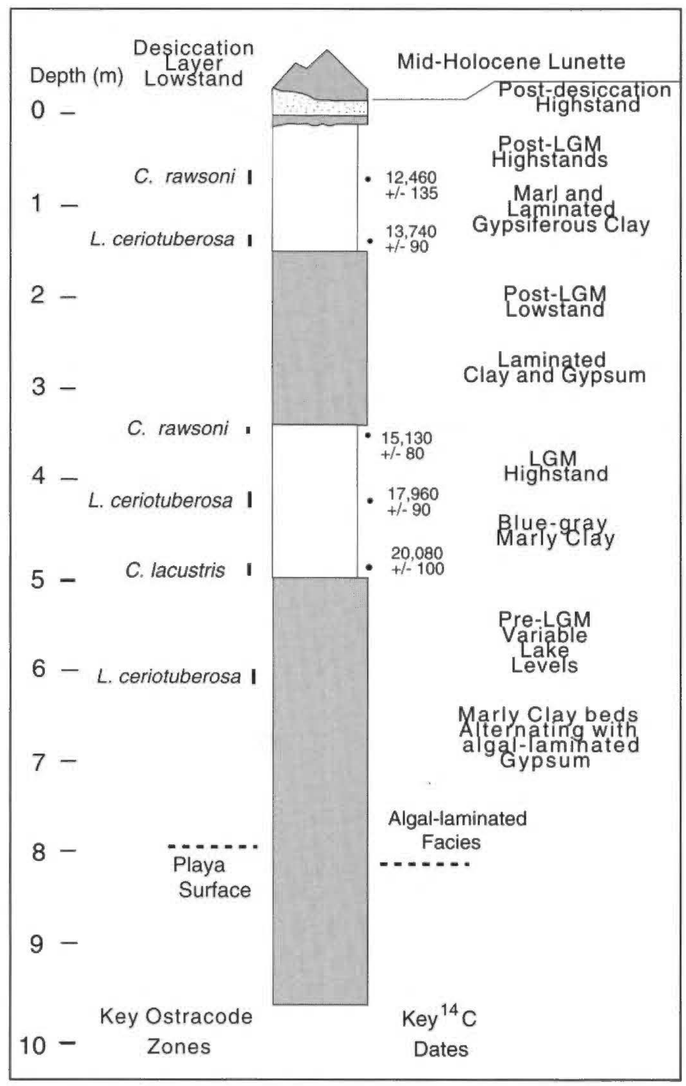

FIGURE 3.2.10. Simplified stratigraphic profile of climatic-stratigraphic units in Estancia lake sediments.

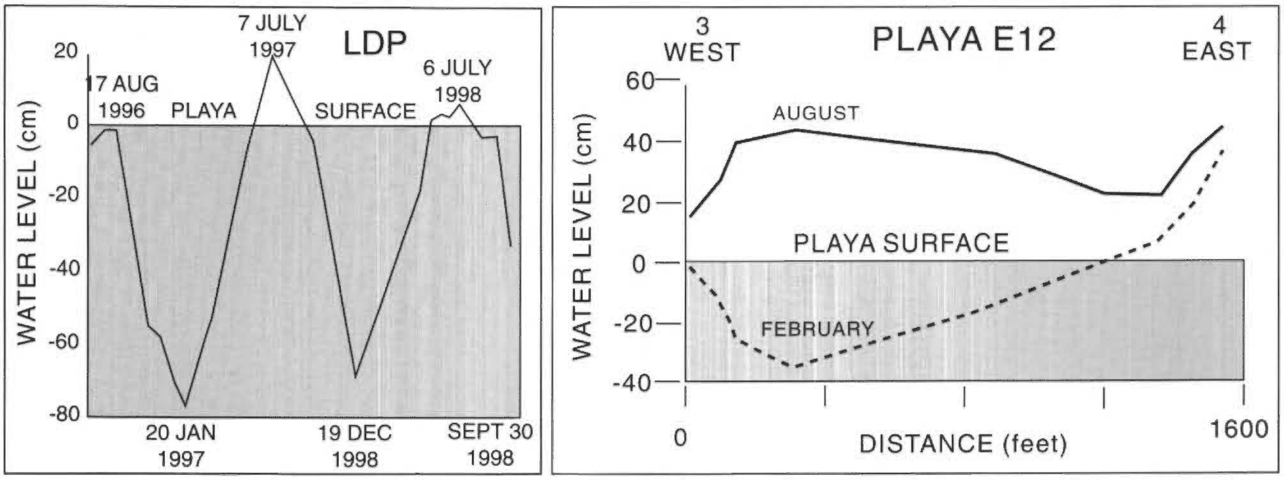

FIGURE 3.2.11. Seasonal changes in water level in piezometers near southern end of LDP, and relation of potentiometric surface to playa surface in a piezometer transect across Playa E12 (transect location in Fig. 3.2.7).

basin hydrology can be found in Shafike and Flanigan (this volume).

Continue west on US-60. Note western arm of Laguna del Perro, 0.5 mi north of highway. **5.7**

78.1 **Pull off of highway for OPTIONAL STOP OS-1**. A reasonably good exposure of the latest Pleistocene lake sequence can be seen by walking about 0.5 mi north of the highway to the nearest, east-facing wall of the deflation-basin. Use of a flat shovel to expose fresh surfaces is advised.

Pleistocene lake sediments. Recognizable stratigraphic units in basin center deposits (Fig. 3.2.10) have approximately the same thickness and composition everywhere in the center of the basin, beneath the area of the minimum pool. Stratigraphic units at Estancia correspond to widely recognized climatic events elsewhere in and beyond western North America, and Bachhuber's (alphabetical) stratigraphic units have been combined into climatic-stratigraphic units that define major highstand and lowstand events (Allen and Anderson, in review).

The desiccated layer (Post-LGM L 3) at the top of the lake-bed sequence at this site was removed by deflation during the first generation of blowouts. Truncated Post-LGM highstand units are largely covered by slope debris, and the surface must be scraped to expose details. A reddish-brown finely laminated unit, about 6.5 ft thick and about 13 ft above the base of the exposure, defines a persistent lowstand (Post-LGM Lowstand 1) that abruptly terminated 5 ka of variable LGM highstands. An underlying, bioturbated, blue-gray clay about 5 ft thick reflects the deeper, fresher, and oxygenated water of LGM highstands. Scraped exposures reveal thin lenses of fine eolian and water-lain gypsum sand that was spread over the lake bottom. The pure white sand fills vertical tubes and burrows in underlying clay. The lower 5 ft contain several alternations of pure clay beds and bundles of algal laminae that are set apart by tenths-of-an-inch-scale laminae of pure, white eolian gypsum (Fig. 3.2.12). These larger bundles mark fluctuations between highstands and lowstands, have an average period of about 1.5–2.0 ka, and correspond to Dansgaard-Oeschger cycles in the latter part of marine isotope Stage III. Smaller bundles of clay and gypsum laminae occur in cycles of a few hundred years.

Reconstructing lake-level and climate fluctuations. Deep pits with vertical faces were dug into the lake beds at this and other localities. Samples were collected every inch and analyzed for several indicators of wet or dry climate episodes (highstand and lowstand conditions), including: (1) degree of lamination and bioturbation (a measure of water depth, salinity, and oxygenation); (2) concentration of calcium carbonate, calcium sulfate, and clay (a function of salinity, shoreline proximity, eolian activity, and water depth); (3) abundance of medium to large grains of detrital quartz (a measure of precipitation, runoff, and active stream discharge into the lake); (4) abundance of several species of ostracodes; salinity tolerance of each species is a measure of duration and degree of lake freshening (wet episodes) and degree of evaporation and concentration (dry episodes); (5) Mg/Ca and Sr/Ca ratio in ostracode valves and marl (a function of salinity and episodes of lake freshening and evaporative drawdown and concentration); and (6) oxygen iso-

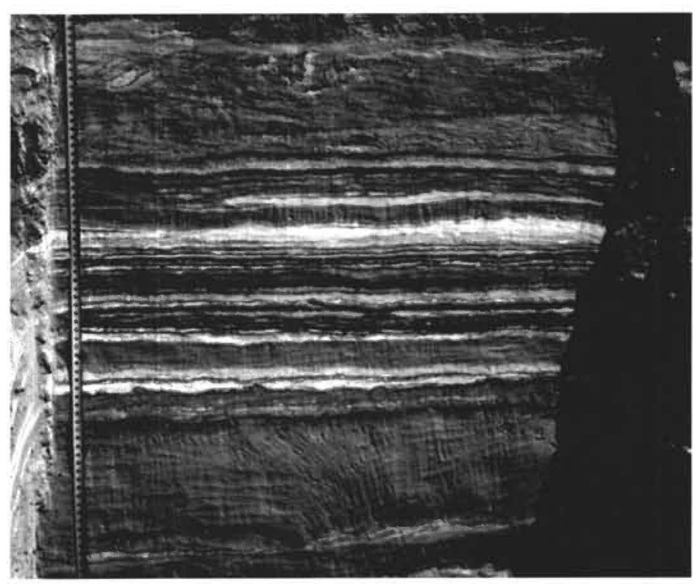

FIGURE 3.2.12 . Exposure of laminated lake sediments in pit excavated into Pre-LGM sediments at LDP (Stop OS1).

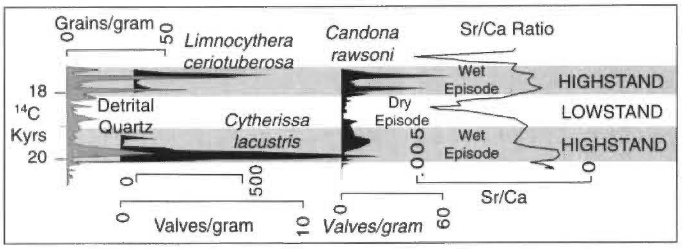

FIGURE 3.2.13. Criteria used to identify wet (highstand) and dry (lowstand) intervals in Estancia lake sediments at the onset of the Last Glacial Maximum.

topic ratio in ostracode valves (a function of evaporative concentration and ground-water and surface-water discharge into the lake).

Identifying wet climate episodes (highstand) is based on having increased bioturbation, higher clay content, presence of detrital quartz, occurrence of ostracodes with low salinity tolerances, and low Sr/Ca and Mg/Ca ratios. Dry episodes (lowstands) are marked by lamination, increased gypsum concentration, absence of detrital quartz, occurrence of ostracodes with high salinity tolerance, and high trace metal ratios.

Figure 3.2.13 shows how some of these parameters were used to identify highstands and lowstands in lake sediments at the onset of the Last Glacial Maximum (LGM). Similar criteria were used to assemble the number and duration of wet and dry episodes (highstands and lowstands) from before the LGM until lake desiccation.

Distinctive zones of ostracodes were used to trace wet and dry episodes (stratigraphic units) to their corresponding shoreline elevation. AMS dating of ostracodes provided the chronology for measuring the timing, duration, abruptness of the wet and dry climate events. The result is the detailed record of changes in lake level fluctuations between ~24 ka and ~12 ka depicted in Figure 3.2.14.

Hydrologic-climatic history of Estancia basin. Past changes in regional and hemispheric climate have been reconstructed, indirectly, in Estancia basin, by compiling a continuous record of changes in the water table (Fig. 3.2.14). The elevation of the water surface reflects a dynamic hydrologic balance between evaporative water loss on one side, and the total of groundwater discharge surface discharge, and precipitation on evaporative surfaces on the other side. Today, recharge of groundwater is mainly in limestone terrain on upper and intermediate slopes in the Manzano Mountains, above ~6600 ft, where annual precipitation ranges from ~18 to 30 in. (NOAA; Tuan, et al., 1973). Precipitation on the valley floor is ~14 in. About 60 % of annual precipitation at lower elevations is from sporadic, summer thunderstorms, accompanied by some local runoff. Under modern climate, little or no surface runoff from elevations above 6600 ft

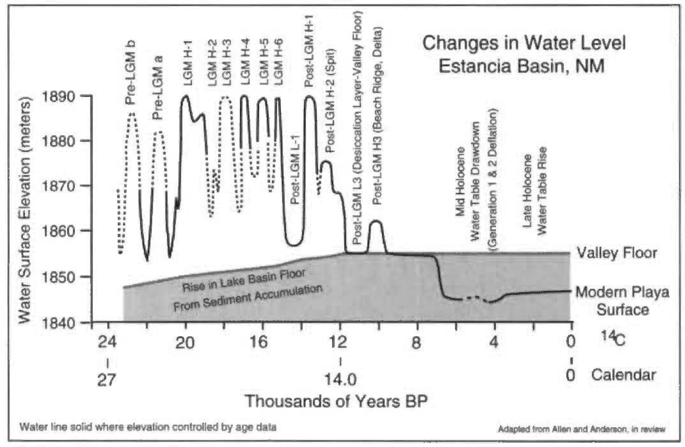

FIGURE 3.2.14. Reconstruction of changes in water level in Estancia basin.

reaches the valley floor. Stream channels around the margin of the basin terminate at the elevation of ~6150 ft, indicating little streamflow since disappearance of the Pleistocene lake. Exceptions are a few streams originating in the Manzano Mountains, which created small deltas and supported a temporary lake rise to 6110 ft at ~10 ka.

At the onset of the LGM the elevation of the hydrologic balance, as reflected in the lake surface, rose ~150 ft above the floor of the basin and fluctuated repeatedly between maximum highstands and a smaller pool that was sustained mainly by groundwater discharge. A record of these lake-level fluctuations was reconstructed by identifying wet and dry climate episodes (highstands and lowstands) from evidence preserved in the lake sediments. At the onset of the Holocene the elevation of the water table fell to the desiccated floor of the Pleistocene lake. Water loss by evaporation was reduced from about 155 mi^2 to less than ~8 mi^2, the surface area of deflating playas, and a new hydrologic balance was struck in which the water level was ~33-ft lower than the old lake floor.

Today, the potentiometic surface in water-bearing units beneath playas is at or slightly above the wet playa surface. The amount of sediment that accumulates within or deflates from a playa basin is linked to the elevation of the wet playa surface. The filling of the playa basins, and the net rise in water elevation during the last few thousand years reflects a new hydrologic balance following the extreme desiccation of the mid-Holocene. Changes in water level during the Holocene have been appended to changes in lake level during the late Pleistocene, and the entire record reflects the basin's hydrologic response to changes in regional climate.

End of Third-day, Trip 2 Road Log.